Manipulating the motion of large neutral molecules

Jochen Küpper,* Frank Filsinger, and Gerard Meijer
Fritz-Haber-Institut der Max-Planck-Gesellschaft, Faradayweg 4–6, 14195 Berlin, Germany

Large molecules have complex potential-energy surfaces with many local minima. They exhibit multiple stereo-isomers, even at very low temperatures. In this paper we discuss the different approaches for the manipulation of the motion of large and complex molecules, like amino acids or peptides, and the prospects of state- and conformer-selected, focused, and slow beams of such molecules for studying their molecular properties and for fundamental physics studies.
Accepted for publication in *Faraday Disc.* **142** (2009)

I. INTRODUCTION

Over the last years there have been tremendous advances in the preparation of cold and ultracold samples of small molecules, either by association of molecules from ultracold atoms, or by direct cooling methods. Using the association technique, ultracold heteronuclear ground-state dimers were recently produced.[1,2] Direct cooling methods allow the preparation of trapped samples of more complex molecules (i. e., ammonia)[3] and they promise possibilities for their extension to large molecules like the "building blocks of life".[4] Recently, we have demonstrated the alternating gradient (AG) deceleration of the prototypical large molecule benzonitrile.[5] Once such molecules are decelerated to a quasi-standstill in the laboratory frame, they can be trapped in ac traps, which have been demonstrated for small molecules in high-field-seeking states.[6,7]

For many applications in physics and chemistry ensembles of large molecules all in one or in a few quantum states would be highly beneficial. For many years, small molecules have been state-selected and focused using static multipole fields.[8,9] For about ten years it is also feasible to change the velocity of small molecules in low-field-seeking states using the Stark decelerator.[10] The produced samples of slow molecules can be trapped in static or dynamic fields, can be injected into storage rings, or can be used for various molecular physics applications.[11]

Larger molecules, however, have practically only high-field-seeking (hfs) states at the relevant electric field strengths. To illustrate this the Stark curves of some low rotational states of benzonitrile (C_7H_5N) are shown in figure 1. In order to focus molecules in these hfs states one would need to create a maximum of electric field in free space, which is not possible according to Maxwell's equations.[8,9] However, large molecules have been deflected using static fields[13,14] and their motion was manipulated in that way in matter-wave interferometry experiments.[15] Moreover, the rotational motion of large molecules has been restricted using brute-force orientation in dc electric fields,[16–18] using laser alignment,[19–21] or using mixed dc and laser fields.[14,22,23]

In order to confine the motion of large molecules, one has to use dynamic focusing in alternating-gradient (AG) setups.[24,25] We have demonstrated that alternating-gradient focusing can be used to focus and decelerate large molecules. In a prototype experiment we have decelerated benzonitrile (C_7H_5N) molecules from a supersonic jet.[5] In similar experiments, we have demonstrated that the frequency characteristics for the dynamic focusing in an AG setup can be used to separate species with distinct mass-to-dipole moment ratios.[26] Equivalent to the m/q-selection of charged particles in a mass spectrometer, these experiments perform an m/μ-selection. We have demonstrated the selection of the cis and trans conformers of 3-aminophenol (C_6H_7NO) and are currently performing first selection experiments on the conformers of biomolecules. Slow, albeit warm, beams of thermally stable, large molecules can also directly emerge from an oven.[27]

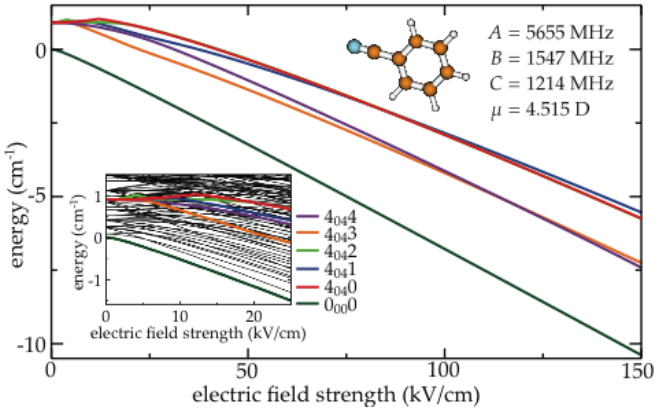

FIG. 1: (Colour online): Energy of selected low rotational states of benzonitrile as a function of electric field strength. In the upper inset the molecular structure of benzonitrile and its relevant molecular parameters are given.[12] In the lower inset, all states with a field-free energy below 1.2 cm^{-1} are shown at smaller field strengths.

The spectroscopic investigation of complex molecules isolated in the gas-phase has also seen big advances over the last decade.[28,29] These advances are largely due to the ability to create intense molecular beams of large molecules and to ingenious multi-resonance laser spectroscopy schemes that allow to disentangle the signatures of different isomers[30] present even in cold molecular beams.[31] However, for many novel studies it would be very advantageous, or even necessary, to separate the

individual isomers, to select quantum states, or to slow down these molecules. There is a large interest in performing coherent x-ray diffractive imaging of biomolecules[32] using novel free-electron-laser x-ray sources. It would be very advantageous to perform initial experiments on well-defined targets: ensembles of molecules all with the same structure (conformation) and all strongly oriented in space. Similar arguments can be made for high-harmonic generation[33] or tomographic orbital reconstruction[34] experiments using (large) molecules.

In this paper we will describe the different experimentally proven methods for the manipulation of the motion of large molecules. We will focus on the manipulation of the translational motion, where we will present detailed descriptions and experimental results obtained in our laboratory. We place special emphasis on the ability to separate conformers with these experiments and will compare the approaches with one another.

II. EXPERIMENTAL APPROACHES

Several complementary experimental approaches for the manipulation of the translation and for the state selection of large neutral molecules exist. Here we limit the discussion to the use of inhomogeneous electric fields, although similar experiments could be performed using magnetic[35–37] or laser fields.[38,39] All these methods rely on the strong cooling provided by supersonic expansions, where rotational and translational temperatures in the moving frame of the molecular beam on the order of 1 K are routinely achieved.[40]

Whereas this article describes the manipulation of the translational motion of molecules, methods to manipulate the rotational motion have also been demonstrated. There are several electric field based methods that are applicable for large molecules, which are generally asymmetric rotors. The conceptionally simplest method to confine the angular distribution of polar molecules is the interaction of the molecular dipole with a strong homogeneous electric field, as proposed independently by Loesch *et al*[16] and by Friedrich and Herschbach.[17] This approach has been experimentally demonstrated many times and is summarised elsewhere.[41,42] This "brute force orientation" of large molecules has been exploited, for example, to determine transition moment angles in the molecular frame.[43,44] Applying strong, non-resonant laser fields to the molecules also provokes angular confinement.[20] The crucial influence of the population of rotational states has been experimentally investigated.[21] Clearly, the state-selection of the lowest rotational states, performed by the experiments described below, allows for considerably stronger degrees of alignment.[14] Recently, strong alignment and orientation by mixed dc electric and laser fields[45,46] has been demonstrated for the large asymmetric top molecule iodobenzene.[14] For a more-in-depth discussion of alignment and orientation the reader is referred to the existing excellent reviews[20,47]

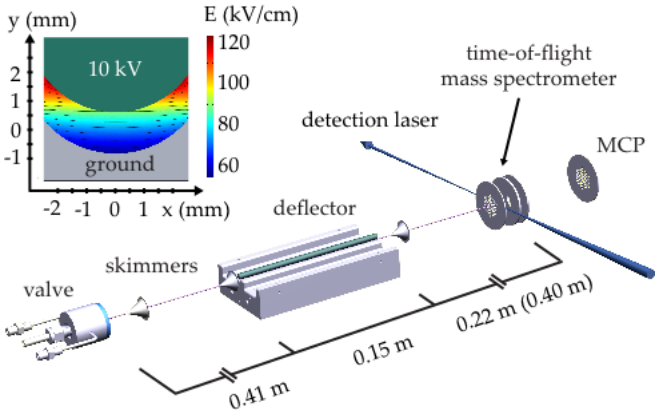

FIG. 2: (Colour online): Experimental setup of the electric m/μ deflector for quantum-state selection of large molecules. An internally cold molecular beam is produced by expanding a mixture of a few percent of the investigated molecule in several bar of rare gas. The resulting supersonic jet is skimmed a few centimetres downstream the nozzle for differential pumping and again about 41 cm downstream the nozzle by a 1 mm diameter skimmer for beam collimation. Then the molecular beam enters the electric deflector, where the inhomogeneous field shown enlarged in the inset provides a force on polar molecules in the vertical direction. Behind the deflector another 1.5 mm skimmer provides further differential pumping for the molecules entering the detection chamber, where the (vertical) deflection profiles can be measured by scanning a pulsed dye laser up and down in an resonance-enhanced multi-photon-ionisation time-of-flight mass-spectrometry detection scheme.

A. Electric beam deflection

1. *General description*

The possibility to deflect polar molecules from a molecular beam using inhomogeneous electric fields was first described by Kallmann and Reiche in 1921.[48,90] Already in 1926 Stern suggested that the technique could be used for the quantum state separation of small diatomic molecules at low temperatures.[49] The electric deflection of a molecular beam was experimentally demonstrated by Wrede – a doctoral student of Otto Stern – in 1927 and the dipole moment of KI was determined.[50] In 1939 Rabi introduced the molecular beam resonance method, by using two deflection elements of oppositely directed gradients in succession to study the quantum structure of atoms and molecules.[51] Already by 1956 a number of different approaches to beam deflection were discussed in Ramsey's textbook.[8] Since then, electric beam deflection has been used extensively, for example, to determine polarisabilities and dipole moments of clusters and molecules.[13,52]

Commonly, the so-called two-wire-field geometry, depicted in figure 2, is used,[8] but more advanced electrode geometries have also been employed, for example, in recent matter-wave interferometry experiments.[15] Nevertheless, the classical two-wire field is widely em-

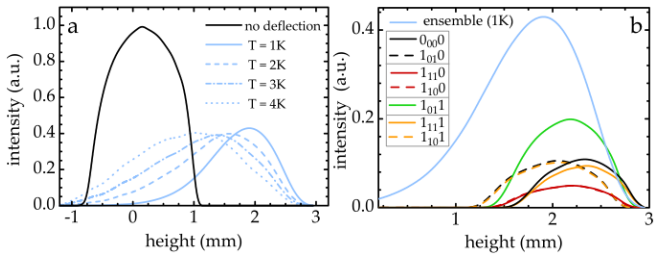

FIG. 3: (Colour online): Deflection profiles a) for molecular beams of benzonitrile at different rotational temperatures and b) for a molecular beam of benzonitrile at 1 K and individual profiles of the lowest energy rotational states. The intensities of all individual states are according to their population at 1 K and are scaled by a factor 10. All calculations are made for the setup shown in figure 2 using a distance from deflector to detector of 22 cm.

ployed, due to its experimental simplicity and the quite good results that can be obtained with it.

2. *Deflection of large molecules*

Using an experimental setup as shown in figure 2 we have, in collaboration with the group of Henrik Stapelfeldt (University of Aarhus, Denmark), deflected large molecules, i. e., iodobenzene (C_6H_5I), and performed laser alignment and mixed-field orientation of the produced state-selected samples.[14] For these studies it was crucial to already start with cold molecular beams as they are produced in high-stagnation-pressure expansions.[53] In figure 3 a the calculated deflection profiles of benzonitrile from molecular beams of varying temperature is shown. For the lowest temperature (1 K) almost the complete beam can be deflected. With increasing temperature, the overall deflection significantly decreases and instead a considerable broadening of the beam is obtained. Due to the large number of quantum states involved we have not performed quantitative calculations for temperatures above 4 K, but approximate calculations suggest that already at 10 K no significant deflection is obtained anymore. In figure 3 b the contribution of the lowest individual rotational states, i. e., all states with $J = 0$ or 1, to the deflection profiles is depicted. These states belong to four different Hamiltonian matrix blocks as shown in the figure legend (see appendix A for details) and the lowest energy states, shown as solid lines in figure 3 b, are all very polar and behave very similar under the influence of the electric field. Especially the states $J_{K_aK_c} = 0_{00}$ and 1_{11} behave extremely similar – they are the ground states of para- and ortho-benzonitrile, respectively – and differ practically only in intensity, which is due to the difference in population.

In any case, using a focused laser or a narrow slit one could perform experiments selectively with the molecular ensemble at a given height. Choosing, for example, a height of $z = 2.7$ mm at 1 K, where the density is 5 % of the density at the peak of the free flight, only a few quantum states are populated, which are all very polar and have very similar effective dipole moments μ_{eff} (the negative gradient of the Stark curve). Therefore, such an ensemble can be strongly oriented using dc electric fields or mixed dc and laser fields.

For cold beams of small molecules with large rotational constants and, therefore, only a few rotational states populated in the molecular beam, this method would allow the preparation of samples of individual rotational states.[49] For low-field-seeking states this can also be achieved using electric multipoles, which also provide transverse focusing,[9,54] or, even cleaner, using the Stark decelerator.[10,55] The deflector, nevertheless, also allows to individually address high-field-seeking states, e. g., absolute ground states.

The large differences between the calculated deflection profiles for benzonitrile at different temperatures also demonstrate that deflection profiles can be used as a sensitive measure of the internal temperatures of molecular beams,[56] especially for low rotational temperatures, where the strongly polar quantum states are populated the most and where meaningful quantum-mechanical calculations can still be performed.

3. *Conformer selection*

For more complex molecules typically multiple conformers are present in a molecular beam.[31] These conformers all have the same mass, but typically exhibit largely different dipole moments. Therefore, one can use the distinct forces exerted on the molecules by inhomogeneous electric fields to spatially separate the molecules based on their m/μ ratios. We have already demonstrated this for 3-aminophenol using dynamic focusing, see section II B and reference 26. Here, we want to discuss the possibilities to use an electric deflector for the same purpose.

In figure 4 the simulated deflection profiles of the cis and trans conformers of 3-aminophenol are shown for the experimental setup described above and the known molecular parameters.[57] For clarity we have assumed equal population of the two species in these simulations; the actual populations can be estimated to be 1:4 for cis-:trans-3-aminophenol from their intensities in electronic spectra. From the simulations at 1 K it is clear that a large fraction of the cis-3-aminophenol conformers can be deflected out of the original beam and even out of the distribution of the trans conformer. Moreover, even at 4 K one can foresee to perform experiments with a pure sample of cis-3-aminophenol. On the other hand, no clean sample of the less polar trans-3-aminophenol conformer can be produced this way. This is even more so, since typically the internal temperatures of the supersonic beams are not thermal[58] and a high-temperature fraction, corresponding to mostly unpolar quantum states, exists. Therefore, in general only one, the most polar conformer,

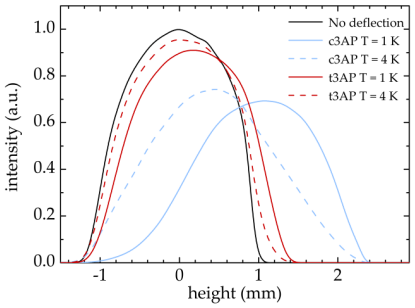

FIG. 4: (Colour online): Simulated deflection profiles of a beam of cis-3-aminophenol (c3AP) and trans-3-aminophenol (t3AP) using the setup described above (with a deflector-to-detector distance of 40 cm) at a voltage of 12 kV applied to the rod and rotational temperatures of 1 and 4 K. In these simulations the populations of cis- and trans-3-aminophenol in the original beam are assumed to be equal.

can be separated from the others. These results should be compared to the demonstrated selection of the conformers of 3-aminophenol using the AG focusing selector described in section II B, where each conformer can be addressed individually.

B. Dynamic focusing selectors

1. *General description*

Whereas deflection experiments allow the spatial dispersion of quantum states, they do not provide any focusing. For small molecules in low-field-seeking states this issue could be resolved using multipole focusers with static electric fields, which were developed independently in Bonn[59,60] and in New York[61,62] in 1954/55. About ten years later, molecular samples in a single rotational state were used for state specific inelastic scattering experiments by the Bonn group[63] and, shortly thereafter, for reactive scattering.[64,65]

However, for large molecules all quantum states are practically hfs at the relevant electric field strengths. Therefore, focusing with static electric fields is not possible. Instead, one has to retreat to dynamic focusing schemes, which are also used in the operation of the LINAC, quadrupole ion guides, or Paul traps for charged particles. Dynamic focusing of neutral polar molecules was described by Auerbach *et al* in 1966.[24] Successively, it was experimentally demonstrated[66–69] and successfully applied in maser experiments.[70,71]

In these early experiments the switching frequency was defined by the beam velocity and the electrode geometry, requiring a setup with alternatingly oriented electric field lenses. Nowadays, however, it is possible to electronically switch the necessary electric fields and one can use, for example, a four-wire setup, shown in figure 5, with varying voltages applied to create the

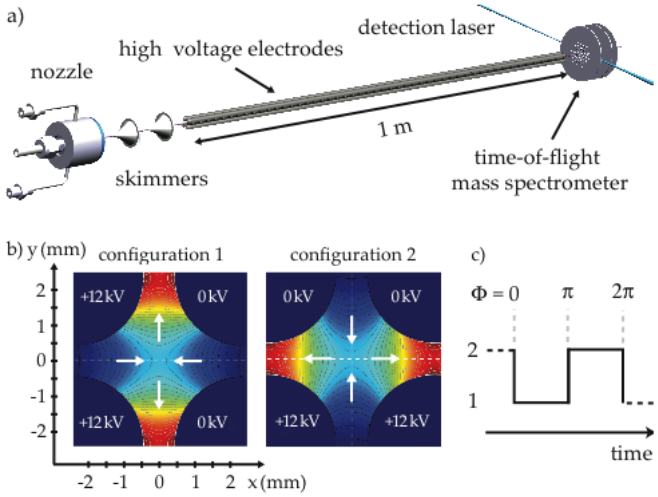

FIG. 5: (Colour online): a) Experimental setup of the dynamic-focusing electric m/μ selector for quantum-state selection of large molecules. An internally cold molecular beam is produced by expanding a mixture of a few percent of the investigated molecule in several bar of rare gas. The resulting supersonic jet is skimmed a few centimetres downstream from the nozzle for differential pumping and again about 18 cm downstream from the nozzle by a xs1 mm diameter skimmer for beam collimation. Then the molecular beam enters the electric selector, where the switched inhomogeneous fields given in the inset (b) provide a focusing force on polar molecules towards the molecular beam axis. The transmission through the selector is monitored in a resonance-enhanced multi-photon-ionisation time-of-flight mass-spectrometry detection scheme. c) Definition of the phase of the switching cycle, where configuration 1 corresponds to focusing in x-direction and 2 to focusing in y-direction for molecules in high-field-seeking states.

necessary alternating gradient focusing at any frequency and always applying the maximum field strength and gradient, i. e., always applying maximal forces.

2. *Focusing of molecules in low- and high-field-seeking states*

In order to characterise the operation of the AG focuser we have performed initial experiments using ammonia (NH_3) in its $J_K = 1_1$ rotational state. NH_3 in this state, the rotational ground state of para ammonia, exhibits a quadratic Stark effect at low and moderate electric field strengths that converges to a linear Stark shift once the Stark energy is comparable to the inversion splitting, as shown in figure 6. Ammonia molecules in the lfs $MK = -1$ component can be focused using a static quadrupole field. This was already exploited by Gordon and Townes in the original demonstration of the MASER[62] and was performed by us for initial optimisation of expansion conditions and laser detection. However, ammonia molecules in both polar quantum states ($MK = -1$ and $+1$) can be confined to the beam axis

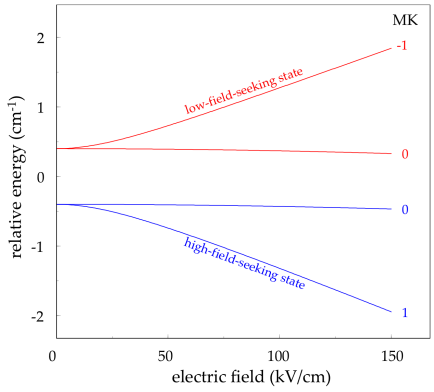

FIG. 6: (Colour online): The energy of ammonia (NH_3) in its $J_K = 1_1$ rotational state as a function of electric field strength (neglecting hyperfine structure).

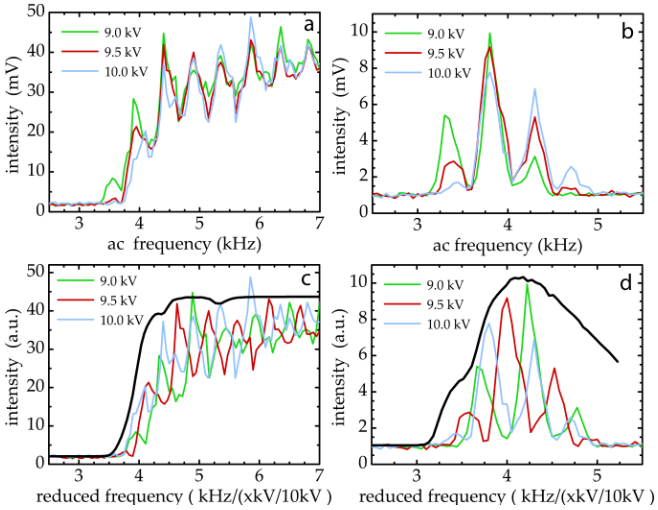

FIG. 7: (Colour online): Measured transmission through the m/μ selector for ammonia in its lfs ($MK = -1$, left graphs) and hfs ($MK = 1$, right graphs) states of the $J_K = 1_1$ rotational state. In the upper plots the experimental transmission as a function of the switching frequency between the two electric field configurations, shown in figure 5 b, is plotted for different applied voltages. The observed strong modulation in all measurements is due to changes in the end-phase of the switching cycle and, therefore, the overlap between the focused detection laser and the molecular packet. The differences in the peak intensities is due to the changed frequency dependence according to the focusing strength at the different voltages. In the lower graphs the same data is plotted as a function of a reduced frequency $\tilde{f} = f/(U/10^4\ \mathrm{V})$ with the applied switching frequency f and voltage U. The envelope of these data nicely represents the simulated overall transmission through the selector (solid black lines), independent of the detection (overlap) function.

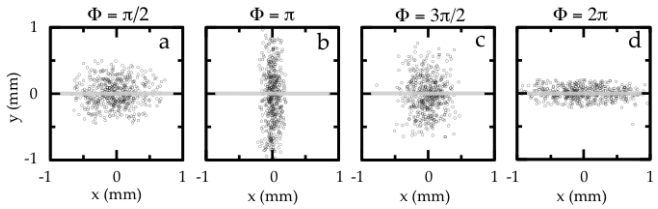

FIG. 8: Transverse phase-space distribution of the molecular packet in the detection region as a function of the end-phase Φ of the switching cycle depicted in figure 5 c. The horizontal grey lines depict the area probed by the focused detection laser.

using AG focusing. This is demonstrated by the measurements in figure 7. Here, the transmissions of NH_3 in its $J_K = 1_1, MK = -1$ and $J_K = 1_1, MK = 1$ states are plotted as a function of the frequency used to switch between the two electric field configurations. The individual states are selectively detected by choosing appropriate 2+1-REMPI transitions. The transmission for the molecules in hfs quantum states (figure 7 b) shows a frequency dependence as expected: At low switching frequencies the molecules are strongly defocused in one direction and lost from the focuser. At high frequency the time averaged potential is approximately flat and no focusing occurs, therefore, the transmission is also low. In between, at the appropriate switching frequency, AG focusing works and the transmission is high. The experimentally measured transmission is strongly modulated in that frequency range. This modulation is due to the overlap between the strongly focused detection laser ($w_L \approx 40\,\mu$m) and the changing shape of the molecular packet. This shape strongly depends on the phase in the switching cycle as depicted in figure 8. Due to the short focusing device – corresponding to a short residence time of the molecules in the device – the start phase, the end phase, and the switching frequency cannot independently be optimised. We chose to optimise the start phase for optimum transmission and then the end phase is determined from the applied switching frequency. In order to reduce these experimental artifacts, we measured the transmission curves for different applied high-voltages U. For comparison the frequencies f of these different measurements are converted to a reduced frequency $\tilde{f} = f/(U/10^4\ \mathrm{V})$ taking into account the effective focusing strength. The resulting transmission characteristics are displayed in figure 7 d. The envelope of these measurements clearly represents the expected overall transmission curve, free of strong effects due to changes in the detection efficiency.

The measurements on ammonia in its lfs $J_K = 1_1$, $MK = -1$ states, shown in figure 7 a and c, demonstrate the versatility of the device. Clear evidence of dynamic focusing is obtained, with similar characteristics as for the hfs states. Two differences in the frequency dependence of the transmission are obvious: at high frequencies the transmission does practically not decrease, and the low-frequency-onset of the transmission curve is shifted towards higher frequencies. The latter demonstrate the quantum state dependence of the process and that, at least in principle, one could use the device to separate the two quantum states. Moreover, since focusing and defocusing forces are interchanged between the lfs and hfs states, the phase effects shown in figure 8 are shifted

by π, which can also be used to discriminate between the two states in laser experiments or by narrow slits in the beam path.

The large transmission at high frequencies is due to the fact that the time-averaged potential (the average of the two potentials in figure 5) is not really flat, but has a minimum of electric field on the molecular beam axis. Therefore, under these conditions molecules in lfs states are focused, whereas molecules in hfs states are defocused. This minimum has a depth of 7.5 kV/cm, corresponding to a 2-dimensional trap depth for ammonia in its lfs state of 0.11 K[91].

3. *Conformer selection*

For given applied voltages the transmission through the selector is a function of the effective dipole moment μ_{eff} of the molecule's quantum state and of the switching frequency f[24,25]: the larger the dipole moment, the higher the optimal switching frequency. Consequently, for a given switching frequency f, the transmission depends on the molecules μ_{eff}. This can, in principle, be exploited for the separation of individual quantum states. As the dipole moments of different conformers of large molecules often vary quite dramatically, one can use the selective focusing to separate the individual conformers from each other. This has been demonstrated for the cis- and trans-conformers of 3-aminophenol.[26]

In comparison to the separation by deflection proposed in section II A 3, the AG focusing selector can provide enhanced transmission for any polar conformer. However, the focused molecules are confined to the molecular beam axis, where there is a background of molecules in unpolar quantum states and of atomic seed gas. In principle, the background could be removed by a beam stop on the molecular beam axis.[9] However, such a beam stop would take away a very large fraction of the beam intensity. Moreover, the central part of the beam is typically also the internally coldest, and, therefore, the most polar one. A similar effect can be obtained by tilting the focuser against the incoming molecular beam axis. We have done this in the selection experiments on 3-aminophenol and it did provide a somewhat improved contrast, although even then a considerable amount of background was observed.[26]

4. *Resolution*

In the conformer selection experiment described above, the focusing selector has been operated under conditions of maximum throughput, the equivalent of a quadrupole *ion guide*. Just like the m/q-resolution of quadrupole mass spectrometers can be improved at the cost of transmission by applying a dc offset, the m/μ-resolution of the focusing selector can be improved at the cost of transmission by changing the duty cycle of the applied high-voltage

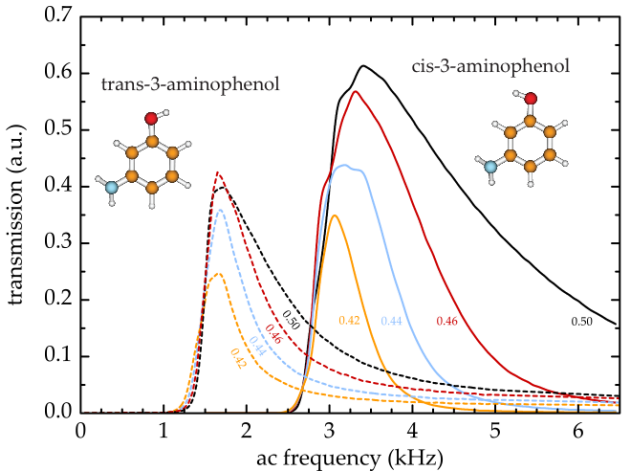

FIG. 9: (Colour online): Calculated transmission through the selector for cis- (full lines) and trans-3-aminophenol (dashed lines) in their rotational ground state for different duty cycles. The duty cycle for each individual simulation is given in the figure.

switching sequence. This effect is demonstrated by the simulations in figure 9, where the transmission as a function of frequency is shown for the ground states of 3-aminophenol for duty cycles $\tau_x/(\tau_x + \tau_y) = 0.5$, 0.46, 0.44, and 0.42, respectively. Here τ_x and τ_y are the fractions of a switching period for which x- and y-focusing are applied (with $\tau_x + \tau_y = 1$). From the calculations it is clear that the changed duty cycle improves the resolution, whereas the intensity decreases simultaneously. In principle, the effect is completely equivalent to the dc offset in a quadrupole guide for charged particles. However, it has to be taken into account that the charged particles experience a harmonic potential inside the guide, whereas the large neutral molecules, discussed here, experience a strongly non-harmonic force. This is due to the often highly non-linear Stark effect (see figure 1) and the higher-order terms in the created electric fields.[25,72] Nevertheless, the effect can be used to separate species with smaller dipole moment differences or, for the same samples, to achieve stronger discrimination between different species. We are currently experimentally verifying these simulations.

It has also to be taken into account, that the molecules experience only a few electric field switching periods inside the current device. Together with the initial spatial spread of the molecular packet, this results in the switching frequency not being well-defined for the molecular ensemble.

In order to be able to routinely operate under conditions with higher resolution we plan to set up a focuser with an improved overall transmission, by scaling up the transverse phase-space acceptance, and a larger residence time, by making the device longer. This should enable us to separate individual conformers of many complex molecules.

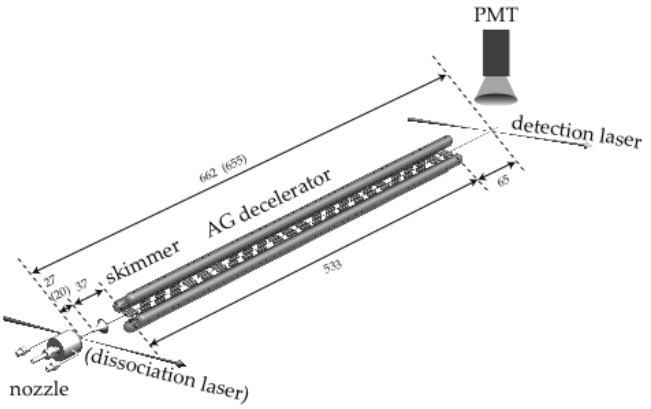

FIG. 10: Experimental setup of the alternating-gradient decelerator. An internally cold molecular beam is produced by expanding a mixture of a few percent of the investigated molecule in approximately 1 bar of rare gas. In experiments with OH, an expansion of HNO_3 is irradiated by a pulsed laser inside the expansion region in order to photodissociate HNO_3 to form OH which is successively cooled in the remaining expansion. The resulting supersonic jet is skimmed a few centimetres downstream from the nozzle for differential pumping and enters the 54 cm long decelerator. The time-resolved transmission of individual quantum states through the decelerator is monitored in a laser-induced-fluorescence detection scheme using a narrow-linewidth continuous-wave dye laser.[5,73]

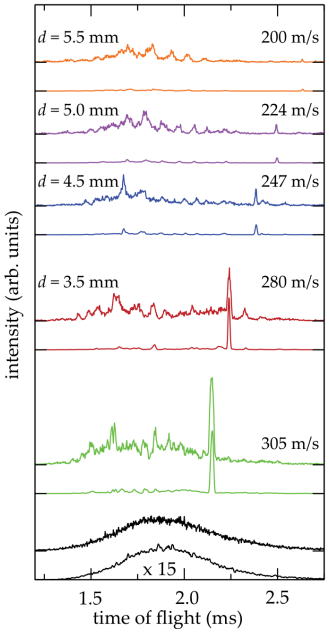

FIG. 11: AG focusing and deceleration of OH in its lfs state from 305 m/s to varying velocities as specified next to the individual measurements. For a deceleration strength of $d = 5.5$ molecular packets with a centre velocity of 200 m/s are obtained.

C. Alternating gradient decelerator

The alternating gradient decelerator, depicted in figure 10, combines the dynamic focusing of the selector with deceleration equivalent to the Stark decelerator[11] and it has been described in detail elsewhere.[24,25] Generally, alternating-gradient deceleration is applicable to molecules in any polar quantum state, i. e., it allows the deceleration of molecules in lfs states and in hfs states. This has been demonstrated for the deceleration of OH radicals in their lfs and hfs components of the $^2\Pi_{3/2}, v = 0, J = 3/2$ Λ-doublet.[73] Experiments on the alternating-gradient deceleration of diatomic molecules in hfs states have also been performed for the diatomic molecules CO*[74] and YbF.[75]

It has also been laid out that, in order to decelerate molecules in lfs states using the AG decelerator, the fields have to be switched on twice per electrode pair – once in between successive pairs in order to provide longitudinal bunching and deceleration, and once inside the electrode pair, in order to provide transverse focusing. In figure 11 a deceleration sequence of OH radicals in their lfs state from 305 to 200 m/s using 27 AG lenses is given. This is the lowest-velocity molecular packet obtained from an AG decelerator so far and it clearly demonstrates the versatility of the AG decelerator. It has to be taken into account, however, that the phase-space acceptance is at least one order of magnitude smaller than for deceleration of OH radicals in their lfs state using the normal Stark decelerator.[73]

For molecules in hfs states the fields are switched on when the molecules are inside the electrode pair (AG lens), where the molecules are focused in transverse direction. When the molecules exit the lens, they are decelerated before the field is switched off again sometime before the molecules reach the minimum of the electric field which is at the centre between two successive lenses. In principle, the focusing works the same way as described for the selector. However, in the decelerator the switching frequency is determined by the distance of successive electrode pairs and the velocity of the molecules and can, therefore, not be varied independently. Moreover, in order to obtain maximal fields on the molecular beam axis for the deceleration process, the fields are created by only two cylindrical electrodes and their geometric orientation defines the focusing and defocusing direction. However, one can change the overall focusing strength for the given geometry/directions by the duration the fields are switched on, or equivalently, by the distance f the molecules travel inside the electrodes. In principle the focusing strength can also be changed by changing the applied voltage. However, this would reduce the maximum field strength and, therefore, the deceleration strength, and it can also not as quickly be adjusted during the experiment.

1. *Alternating gradient deceleration of large molecules*

The experimental setup of the alternating gradient decelerator is shown in figure 10. Using this setup we

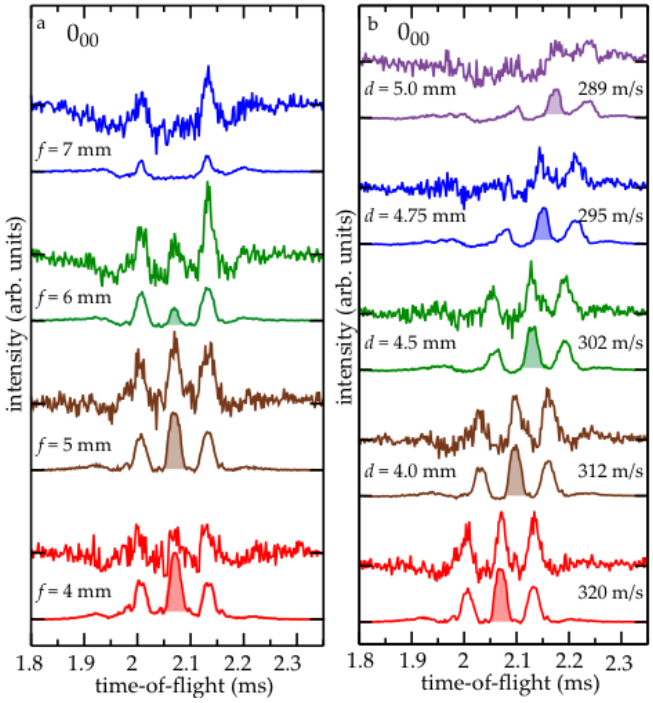

FIG. 12: (Colour online): Alternating-gradient focusing and deceleration of benzonitrile from a molecular beam of 320 m/s.[5] In the left column no overall deceleration is performed and the effects of a changing focusing strength are demonstrated. In the right column packets of benzonitrile molecules are decelerated from 320 m/s to successively lower final velocities as indicated in the figure.

have AG focused and decelerated benzonitrile in its absolute ground state, and the obtained difference-time-of-flight profiles (see reference 5 for details) are shown in figure 12. Figure 12 a illustrates the focusing behavior of the 0_{00} ground state of benzonitrile for a constant velocity of the synchronous molecule of 320 m/s. The high voltages are switched on symmetrically around the centers of the AG lenses. Therefore, the molecular packet is focused in both transverse directions as well as in the longitudinal direction (bunching), but no change of the synchronous velocity occurs. In the experiments three packets of focused molecules are observed. The central peaks of the TOF distributions occur 2.07 ms after the molecules exit the nozzle. These packets contain the synchronous molecule. Hereafter, they are referred to as the "synchronous packets", and they are shaded in the simulated TOF distributions. The peaks at earlier and later arrival times correspond to molecular packets leading and trailing the synchronous packet by one AG lens (or 20 mm), respectively. These packets are also focused in all three dimensions. However, due to the lens pattern in our setup, they experience only 2/3 of the lenses at high voltage. This results in a reduced overall focusing for these packets.

For the focusing of the 0_{00} state it is seen that the synchronous packet is most intense for a focusing length of f = 5 mm. Under these conditions approximately 10^5 molecules per quantum state per pulse are confined in the phase-stable central peak, corresponding to a density of 10^8 cm^{-3}. For smaller focusing lengths a shallower time-averaged confinement potential is created, and less molecules are guided through the decelerator. For larger focusing lengths the molecular packet is over-focused, also resulting in a decreased transmission. For f = 7 mm the over-focusing is so severe that the synchronous packet completely disappears. As expected, the non-synchronous packets benefit from the increased focusing lengths.

Figure 12 b presents the results for the deceleration of benzonitrile in its 0_{00} state. The bottommost (red) trace shows focusing experiments for a constant velocity of the synchronous molecule of 320 m/s using the optimum focusing lengths. All other traces show experiments in which the synchronous packet is decelerated from 320 m/s to successively lower velocities, resulting in later arrival times at the detector. In these experiments the deceleration strength d is given as the position on the molecular beam axis behind the centre of the AG lens, where the electric field is switched off. Using d = 5 mm, the packet is decelerated to 289 m/s, corresponding to a reduction of the kinetic energy by 18 %. The observed intensities of the non-synchronous packets decrease faster upon increasing d. Because the molecules in these packets miss every third deceleration stage, their trajectories are not stable and they are only observed due to the finite length of the decelerator. When deceleration to lower velocities is performed by increasing d the signal intensity decreases due to the reduction in phase-space acceptance. However, one could also decelerate to lower velocities by increasing the number of AG lenses for a given value of d. In this case, in principle, no decrease in the intensity of the synchronous packet is expected due to the phase stability of the deceleration process.[25] For all deceleration measurements, the relative intensities and the arrival times of the molecular packets at the detector are nicely reproduced by the trajectory simulations.

2. *Towards the trapping of large molecules*

Once large molecules in polar quantum states are decelerated down to slow velocities, i. e., below approximately 25 m/s for molecules like benzonitrile or 3-aminophenol, they can be confined in ac electric traps. Such traps have already been demonstrated for slow ammonia molecules in hfs states,[6,7,76] which were produced from Stark decelerated ammonia in lfs states *via* a microwave transition.[77] Trapping lifetimes will be limited by collisions with background gas, by blackbody radiation,[78] and by non-adiabatic following of Stark curves. Even though the collisional cross sections for losses due to background gas will be different for large molecules compared to the ones for small molecules, the effects should be small. Nonadiabatic dynamics on the Stark potential energy curves do

not occur for the lowest quantum state. For higher states it can be avoided, at least for low-lying rotational states, by providing finite minimum electric field strength on the order of 10 kV/cm. This also efficiently prohibits Majorana transitions. Since ac traps must provide a saddle point in the trap centre this requirement is practically automatically fulfilled.

The blackbody-radiation lifetimes of individual states can be calculated from the radiation density and the possible transitions. For the rovibronic ground state ($J_{K_aK_c} = 0_{00}$) two types of transitions have to be taken into account: rotational excitation into the rotational excited states that can be reached by an allowed transition and vibrational excitations. We have performed the calculation for the lifetime of benzonitrile in its rovibronic ground state as an example of a prototypical large polar molecule. At 300 K the rotational transition rate for the $1_{01} \leftarrow 0_{00}$ rotational *a*-type transition at 2.76 GHz[12] is 10^{-5} Hz. In order to estimate the vibrational transition rate, we have performed a geometry optimisation and normal coordinate analysis at the B3LYP/aug-cc-pVTZ level of theory using Gaussian 2003,[79] which yields transition strengths for all 33 fundamental transitions. This results in an overall rate for loss of ground state molecules due to blackbody radiation at room temperature (300 K) of less than 1/4 Hz. The resulting trapping lifetime of 4 s is larger than currently achieved trapping times of small molecules in ac traps[6,7,76,80] and does not pose a major restriction on the trapping of such large molecules. However, the major loss rate is due to low-frequency vibrations with transition frequencies between 400 and 800 cm^{-1}. Therefore, the lifetime would increase to several hundred seconds when the trapping environment is cooled to liquid nitrogen temperatures (77 K). Moreover, one has to consider that many of the final states are also confined in the ac trap and, eventually, population will also be transferred back to the ground state. This shows that large molecules can be confined in traps once they are decelerated to slow enough velocities and that, while thermalization due to blackbody radiation has to be considered at room temperature, it will not prohibit trapping of large molecules and it is negligible at liquid nitrogen temperatures.

3. *Conformer selection with the alternating-gradient decelerator*

Generally, the quantum-state selectivity of the AG decelerator provides for the possibility to prepare clean samples of individual conformers of large molecules. Similar to the AG focuser, any polar conformer can be addressed. Additionally, even without the deceleration to very slow velocities the reduced velocity and the correspondingly longer flight-times to the detector allow for a practically complete temporal separation of the accepted molecules from the remaining beam. Therefore, the AG decelerator provides, in principle, the best selectivity of different conformers present in an molecular beam. Decelerating a single conformer to slow velocities and successively trapping it in ac traps provides additional selectivity and allows for the separation of quantum states and conformers with quite similar m/μ ratios. However, this strong selectivity comes at the price of a more complicated experimental setup.

III. CONCLUSIONS

We have compared and demonstrated different experimental approaches for the quantum-state selective manipulation of the motion of polar molecules. All methods are generally applicable for molecules in low- and high-field seeking states. However, the methods presented here are well adapted to the manipulation of large molecules, where all quantum states are high-field seeking.

Generally, all the different techniques described allow the spatial separation of different isomers of neutral species. While we have demonstrated this already for 3-aminophenol using the m/μ selector, it is clear that the quantum state selectivity of the deflector and the AG decelerator can be exploited in very much the same way. Moreover, both these alternative techniques can provide background free samples of large molecules. Generally, each approach has its advantages and disadvantages, which shall be summarised here.

Using the deflector one disperses quantum states of particles of identical mass according to their effective dipole moments μ_{eff}, with the most polar states deflected the most. Therefore, using focused lasers or narrow slits for spatial discrimination of the sample, one can perform experiments using samples of these most polar quantum states. Contrary to the AG selector, these are pure samples without any background from unpolar states or conformers, or seed gas, as is shown by the simulations for cis and trans 3-aminophenol in figure 4. In principle this background in experiments with the AG focuser can be removed by bending or tilting the device with respect to the molecular beam axis or by placing a beam-stop on the molecular beam axis in order to remove particles unaffected by the electric fields, but these changes will also considerably reduce the transmission of the selected particles. The AG focuser, however, has the advantage that it allows the selection of any conformer whose dipole moment differs (enough) from the other conformers.

Background reduction can, of course, also be performed in time. If one uses the alternating gradient decelerator to slow the accepted molecular packet – containing only a single conformer – down to reach the detector only after the original pulse has passed, one can also perform practically background free experiments with the accepted packets. Of course, the ultimate experiment in that respect would be the deceleration and subsequent trapping of a single conformer.

For future proof-of-principle experiments on single

conformers the deflector is surely the most promising setup. It is the simplest of the presented techniques, and it provides a background-free sample of the most polar quantum states of the most polar isomer, the states that can also be manipulated the strongest in successive laser or dc electric field experiments, like mixed field orientation.[14] However, if one wants to employ the separation in routine experiments where specific or multiple isomers must be addressed individually, generally dynamic focusing is obligatory in order to obtain enriched samples of any but the most polar conformer. Whether the experiments requires really pure samples or not determines whether the simpler focuser or the very complex decelerator shall be used.

Whereas the discussions of m/μ selection in this manuscript were restricted to the separation of isomers of molecules (fixed m), the selection can of course also be used to separate species from any other mixture based on the m/μ-ratio, i. e., to separate polar clusters from the typically very broad size distributions.

Generally, the clean, well-defined samples provided by these experiments could aid or even just allow novel experiments with complex molecules, for instance, femtosecond pump-probe measurements, x-ray or electron diffraction in the gas-phase, or tomographic reconstructions of molecular orbitals. Such samples could also be very advantageous for metrology applications, such as, for example, matter-wave interferometry or the search for electroweak interactions in chiral molecules.

APPENDIX A: STARK ENERGIES OF ASYMMETRIC ROTORS

In this section we want to summarise the details of the calculations of adiabatic energy curves for asymmetric top molecules. The Hamiltonian matrix is set up in the basis of symmetric top wavefunctions. For the asymmetric rotor in an electric field only M is a good quantum number, as K is mixed by the molecular asymmetry and J is mixed by the field. Therefore, one can treat the different M levels individually, but needs to set up the M matrices including all J and K levels. For the accurate description of higher rotational states it is also important to include centrifugal distortion constants. The Hamiltonian H of an asymmetric rotor molecule with dipole moment $\vec{\mu}$ in an electric field of strength E might be written as the sum of the Hamiltonian H_{rot} of an asymmetric rotor in free space and the contribution due to the Stark effect H_{Stark} as

$$H = H_{\text{rot}} + H_{\text{Stark}}$$

Following references 81 and 82, the corresponding matrix elements, using symmetric rotor basis functions, representation I^r, and Watson's A-reduction,[81] are:

$$\begin{aligned}
\langle JKM \mid H_{\text{rot}} \mid JKM\rangle &= \frac{B+C}{2}\left(J(J+1)-K^2\right) + AK^2 \\
&\quad - \Delta_J J^2(J+1)^2 - \Delta_{JK} J(J+1)K^2 - \Delta_K K^4 \\
\langle JK \pm 2M \mid H_{\text{rot}} \mid JKM\rangle &= \left(\frac{B-C}{4} - \delta_J J(J+1) - \frac{\delta_K}{2}\left((K\pm 2)^2 + K^2\right)\right) \\
&\quad \cdot \sqrt{J(J+1)-K(K\pm 1)}\,\sqrt{J(J+1)-(K\pm 1)(K\pm 2)} \\
\langle JKM \mid \mu_a \mid JKM\rangle &= -\frac{MK}{J(J+1)}\mu_a E \\
\langle J+1KM \mid \mu_a \mid JKM\rangle &= \langle JKM \mid \mu_a \mid J+1KM\rangle \\
&= -\frac{\sqrt{(J+1)^2-K^2}\,\sqrt{(J+1)^2-M^2}}{(J+1)\sqrt{(2J+1)(2J+3)}}\mu_a E \\
\langle JK \pm 1M \mid \mu_b \mid JKM\rangle &= -\frac{M\sqrt{(J\mp K)(J\pm K+1)}}{2J(J+1)}\mu_b E \\
\langle J+1K \pm 1M \mid \mu_b \mid JKM\rangle &= \langle JK \pm 1M \mid \mu_b \mid J+1KM\rangle \\
&= \pm\frac{\sqrt{(J\pm K+1)(J\pm K+2)}\,\sqrt{(J+1)^2-M^2}}{2(J+1)\sqrt{(2J+1)(2J+3)}}\mu_b E \\
\langle JK \pm 1M \mid \mu_c \mid JKM\rangle &= \pm i\frac{M\sqrt{(J\mp K)(J\pm K+1)}}{2J(J+1)}\mu_c E \\
\langle J+1K \pm 1M \mid \mu_c \mid JKM\rangle &= \langle JK \pm 1M \mid \mu_c \mid J+1KM\rangle \\
&= -i\frac{\sqrt{(J\pm K+1)(J\pm K+2)}\,\sqrt{(J+1)^2-M^2}}{2(J+1)\sqrt{(2J+1)(2J+3)}}\mu_c E
\end{aligned}$$

For the correct assignment of the states to the "adiabatic quantum number labels" $\tilde{J}\tilde{K}_a\tilde{K}_c\tilde{M}$, i. e., to the adiabatically corresponding field-free rotor states, one has to classify the states according to their character in the *electric field symmetry group*.[83,84] This symmetry classification is performed by applying a Wang transformation[85] to the Hamiltonian matrix. If the molecule's dipole moment is along one of the principal axes of inertia, the matrix will be block diagonalised by this transformation according to the remaining symmetry in the field and the blocks are treated independently. For arbitrary orientation of the dipole moment in the inertial frame of the molecule the full matrix must be diagonalised. In any case, this process ensures that all states (eigenvalues and eigenvectors) obtained from a single matrix diagonalisation do have the same symmetry, and, therefore, no real crossings between these states can occur. Therefore, by sorting the resulting levels by energy and assigning quantum number labels in the same order as for the field-free states of the same symmetry yields the correct adiabatic labels.

These calculations are performed for a number of electric field strengths – typically in steps of 1 kV/cm from 0 kV/cm to 250 kV/cm – and the resulting energies are stored for later use in simulations using the libcoldmol program package.[86]

* Electronic address: jochen@fhi-berlin.mpg.de

1 K.-K. Ni, S. Ospelkaus, M. H. G. de Miranda, A. Pe'er, B. Neyenhuis, J. J. Zirbel, S. Kotochigova, P. S. Julienne, D. Jin, and J. Ye, *Science*, 2008, **322**, 231.

2 J. Deiglmayr, A. Grochola, M. Repp, K. Mörtlbauer, C. Glück, J. Lange, O. Dulieu, R. Wester, and M. Weidemüller, *Phys. Rev. Lett.*, 2008, **101**, 133004.

3 H. L. Bethlem, G. Berden, F. M. H. Crompvoets, R. T. Jongma, A. J. A. van Roij, and G. Meijer, *Nature*, 2000, **406**, 491–494.

4 R. Weinkauf, J. Schermann, M. S. de Vries, and K. Kleinermanns, *Eur. Phys. J. D*, 2002, **20**, 309–316.

5 K. Wohlfart, F. Grätz, F. Filsinger, H. Haak, G. Meijer, and J. Küpper, *Phys. Rev. A*, 2008, **77**, 031404(R).

6 J. van Veldhoven, H. L. Bethlem, and G. Meijer, *Phys. Rev. Lett.*, 2005, **94**, 083001.

7 M. Schnell, P. Lützow, J. van Veldhoven, H. L. Bethlem, J. Küpper, B. Friedrich, M. Schleier-Smith, H. Haak, and G. Meijer, *J. Phys. Chem. A*, 2007, **111**, 7411–7419.

8 N. F. Ramsey, *Molecular Beams*, The International Series of Monographs on Physics, Oxford University Press, London, GB, 1956.

9 J. Reuss In Scoles,[40] chapter 11, pp. 276–292.

10 H. L. Bethlem, G. Berden, and G. Meijer, *Phys. Rev. Lett.*, 1999, **83**, 1558–1561.

11 S. Y. T. van de Meerakker, H. L. Bethlem, and G. Meijer, *Nature Phys.*, 2008, **4**, 595.

12 K. Wohlfart, M. Schnell, J.-U. Grabow, and J. Küpper, *J. Mol. Spec.*, 2008, **247**, 119–121.

13 M. Broyer, R. Antoine, I. Compagnon, D. Rayane, and P. Dugourd, *Phys. Scr.*, 2007, **76**, C135–C139.

14 L. Holmegaard, J. H. Nielsen, I. Nevo, H. Stapelfeldt, F. Filsinger, J. Küpper, and G. Meijer, *Phys. Rev. Lett.*, 2009, **102**, 023001.

15 M. Berninger, A. Stefanov, S. Deachapunya, and M. Arndt, *Phys Rev A*, 2007, **76**, 013607.

16 H. J. Loesch and A. Remscheid, *J. Chem. Phys.*, 1990, **93**, 4779.

17 B. Friedrich and D. R. Herschbach, *Nature*, 1991, **353**, 412–414.

18 P. A. Block, E. J. Bohac, and R. E. Miller, *Phys. Rev. Lett.*, 1992, **68**, 1303–1306.

19 B. Friedrich and D. Herschbach, *Phys. Rev. Lett.*, 1995, **74**, 4623–4626.

20 H. Stapelfeldt and T. Seideman, *Rev. Mod. Phys.*, 2003, **75**, 543–557.

21 V. Kumarappan, C. Z. Bisgaard, S. S. Viftrup, L. Holmegaard, and H. Stapelfeldt, *J. Chem. Phys.*, 2006, **125**, 194309.

22 U. Buck and M. Fárník, *Int. Rev. Phys. Chem.*, 2006, **25**, 583–612.

23 S. Minemoto, H. Nanjo, H. Tanji, T. Suzuki, and H. Sakai, *J. Chem. Phys.*, 2003, **118**, 4052–4059.

24 D. Auerbach, E. E. A. Bromberg, and L. Wharton, *J. Chem. Phys.*, 1966, **45**, 2160.

25 H. L. Bethlem, M. R. Tarbutt, J. Küpper, D. Carty, K. Wohlfart, E. A. Hinds, and G. Meijer, *J. Phys. B*, 2006, **39**, R263–R291.

26 F. Filsinger, U. Erlekam, G. von Helden, J. Küpper, and G. Meijer, *Phys. Rev. Lett.*, 2008, **100**, 133003.

27 S. Deachapunya, P. J. Fagan, A. G. Major, E. Reiger, H. Ritsch, A. Stefanov, H. Ulbricht, and M. Arndt, *Eur. Phys. J. D*, 2008, **46**, 307–313.

28 J. P. Simons, *Phys. Chem. Chem. Phys.*, 2004, **6**, E7.

29 M. S. de Vries and P. Hobza, *Annu. Rev. Phys. Chem.*, 2007, **58**, 585–612.

30 R. D. Suenram and F. J. Lovas, *J. Am. Chem. Soc.*, 1980, **102**, 7180–7184.

31 T. R. Rizzo, Y. D. Park, L. Peteanu, and D. H. Levy, *J. Chem. Phys.*, 1985, **83**, 4819–4820.

32 R. Neutze, R. Wouts, D. van der Spoel, E. Weckert, and J. Hajdu, *Nature*, 2000, **406**, 752–757.

33 J. Itatani, D. Zeidler, J. Levesque, M. Spanner, D. M. Villeneuve, and P. B. Corkum, *Phys. Rev. Lett.*, 2005, **94**.

34 J. Itatani, J. Levesque, D. Zeidler, H. Niikura, H. Pépin, J. C. Kieffer, P. B. Corkum, and D. M. Villeneuve, *Nature*, 2004, **432**, 867–871.

35 W. Gerlach and O. Stern, *Z. Phys.*, 1922, **9**, 349–352.

36 N. Vanhaecke, U. Meier, M. Andrist, B. H. Meier, and F. Merkt, *Phys. Rev. A*, 2007, **75**, 031402(R).

37 E. Narevicius, A. Libson, C. G. Parthey, I. Chavez, J. Narevicius, U. Even, and M. G. Raizen, *Phys. Rev. Lett.*, 2008, **100**, 093003.

38 B. S. Zhao, H. S. Chung, K. Cho, S. H. Lee, S. Hwang, J. Yu, Y. H. Ahn, J. Y. Sohn, D. S. Kim, W. K. Kang, and D. S. Chung, *Phys. Rev. Lett.*, 2000, **85**, 2705–2708.

39 R. Fulton, A. I. Bishop, and P. F. Barker, *Phys. Rev. Lett.*, 2004, **93**, 243004.

40 ed. G. Scoles, *Atomic and molecular beam methods*, Vol. 1, Oxford University Press, New York, NY, USA, 1988.

41 H. J. Loesch, *Annu. Rev. Phys. Chem.*, 1995, **46**, 555–594.

42 W. Kong, *Int. J. Mod. Phys. B*, 2001, **15**, 3471–3502.

43 K. J. Castle and W. Kong, *J. Chem. Phys.*, 2000, **112**, 10156–10161.

44 F. Dong and R. E. Miller, *Science*, 2002, **298**, 1227–1230.

45 B. Friedrich and D. Herschbach, *J Chem Phys*, 1999, **111**, 6157.

[46] B. Friedrich and D. Herschbach, *J. Phys. Chem. A*, 1999, **103**, 10280–10288.
[47] T. Seideman and E. Hamilton, *Adv Atom Mol Opt Phy*, 2005, **52**, 289–329.
[48] H. Kallmann and F. Reiche, *Z. Phys.*, 1921, **6**, 352–375.
[49] O. Stern, *Z. Phys.*, 1926, **39**, 751–763.
[50] E. Wrede, *Z. Phys.*, 1927, **44**, 261–268.
[51] I. I. Rabi, S. Millman, P. Kusch, and J. R. Zacharias, *Phys. Rev.*, 1939, **55**, 526–535.
[52] R. Moro, X. Xu, S. Yin, and W. A. de Heer, *Science*, 2003, **300**, 1265–1269.
[53] M. Hillenkamp, S. Keinan, and U. Even, *J. Chem. Phys.*, 2003, **118**, 8699–8705.
[54] S. Stolte In Scoles,[40] chapter 25, pp. 631–652.
[55] S. Y. T. van de Meerakker and G. Meijer, *Faraday Disc.*, 2009, **142**, in preparation.
[56] R. Moro, J. Bulthuis, J. Heinrich, and V. V. Kresin, *Phys. Rev. A*, 2007, **75**, 013415.
[57] F. Filsinger, K. Wohlfart, M. Schnell, J.-U. Grabow, and J. Küpper, *Phys. Chem. Chem. Phys.*, 2008, **10**, 666–673.
[58] Y. R. Wu and D. H. Levy, *J. Chem. Phys.*, 1989, **91**, 5278–5284.
[59] H. G. Bennewitz and W. Paul, *Z. Phys.*, 1954, **139**, 489.
[60] H. G. Bennewitz, W. Paul, and C. Schlier, *Z. Phys.*, 1955, **141**, 6.
[61] J. P. Gordon, H. J. Zeiger, and C. H. Townes, *Phys. Rev.*, 1954, **95**, 282–284.
[62] J. P. Gordon, H. J. Zeiger, and C. H. Townes, *Phys. Rev.*, 1955, **99**, 1264–1274.
[63] H. G. Bennewitz, K. H. Kramer, J. P. Toennies, and W. Paul, *Z. Phys.*, 1964, **177**, 84.
[64] P. R. Brooks and E. M. Jones, *J. Chem. Phys.*, 1966, **45**, 3449.
[65] R. J. Beuhler, R. B. Bernstein, and K. H. Kramer, *J. Am. Chem. Soc.*, 1966, **88**, 5331.
[66] D. Kakati and D. C. Lainé, *Phys. Lett. A*, 1967, **24**, 676.
[67] D. Kakati and D. C. Lainé, *Phys. Lett. A*, 1969, **28**, 786.
[68] F. Günther and K. Schügerl, *Z. Phys. Chem.*, 1972, **80**, 155.
[69] A. Lübbert, G. Rotzoll, and F. Günther, *J. Chem. Phys.*, 1978, **69**, 5174–5179.
[70] D. Kakati and D. C. Lainé, *J. Phys. E*, 1971, **4**, 269.
[71] D. C. Lainé and R. C. Sweeting, *Entropie*, 1973, **42**, 165.
[72] M. R. Tarbutt and E. A. Hinds, *New J. Phys.*, 2008, **10**, 073011.
[73] K. Wohlfart, F. Filsinger, F. Grätz, J. Küpper, and G. Meijer, *Phys. Rev. A*, 2008, **78**, 033421.
[74] H. L. Bethlem, A. J. A. van Roij, R. T. Jongma, and G. Meijer, *Phys. Rev. Lett.*, 2002, **88**, 133003.
[75] M. R. Tarbutt, H. L. Bethlem, J. J. Hudson, V. L. Ryabov, V. A. Ryzhov, B. E. Sauer, G. Meijer, and E. A. Hinds, *Phys. Rev. Lett.*, 2004, **92**, 173002.
[76] H. L. Bethlem, J. van Veldhoven, M. Schnell, and G. Meijer, *Phys. Rev. A*, 2006, **74**, 063403.
[77] J. van Veldhoven, J. Küpper, H. L. Bethlem, B. Sartakov, A. J. A. van Roij, and G. Meijer, *Eur. Phys. J. D*, 2004, **31**, 337–349.
[78] S. Hoekstra, J. J. Gilijamse, B. Sartakov, N. Vanhaecke, L. Scharfenberg, S. Y. T. van de Meerakker, and G. Meijer, *Phys. Rev. Lett.*, 2007, **98**, 133001.
[79] M. J. Frisch, G. W. Trucks, H. B. Schlegel, G. E. Scuseria, M. A. Robb, J. R. Cheeseman, J. J. A. Montgomery, T. Vreven, K. N. Kudin, J. C. Burant, J. M. Millam, S. S. Iyengar, J. Tomasi, V. Barone, B. Mennucci, M. Cossi, G. Scalmani, N. Rega, G. A. Petersson, H. Nakatsuji, M. Hada, M. Ehara, K. Toyota, R. Fukud, J. Hasegawa, M. Ishida, T. Nakajima, Y. Honda, O. Kitao, H. Nakai, M. Klene, X. Li, J. E. Knox, H. P. Hratchian, J. B. Cross, V. Bakken, C. Adamo, J. Jaramillo, R. Gomperts, R. E. Stratmann, O. Yazyev, A. J. Austin, R. Cammi, C. Pomelli, J. W. Ochterski, P. Y. Ayala, K. Morokuma, G. A. Voth, P. Salvador, J. J. Dannenberg, V. G. Zakrzewski, S. Dapprich, A. D. Daniels, M. C. Strain, O. Farkas, D. K. Malick, A. D. Rabuck, K. Raghavachari, J. B. Foresman, J. V. Ortiz, Q. Cui, A. G. Baboul, S. Clifford, J. Cioslowski, B. B. Stefanov, G. Liu, A. Liashenko, P. Piskorz, I. Komaromi, R. L. Martin, D. J. Fox, T. Keith, M. A. Al-Laham, C. Y. Peng, A. Nanayakkara, M. Challacombe, P. M. W. Gill, B. Johnson, W. Chen, M. W. Wong, C. Gonzalez, and J. A. Pople, Gaussian 03, Gaussian, Inc., Wallingford CT, 2004.
[80] J. van Veldhoven *AC trapping and high-resolution spectroscopy of ammonia molecules* Ph. D. thesis, Radboud Universiteit Nijmegen, The Netherlands, 2006.
[81] J. K. G. Watson in *Vibrational Spectra and Structure*, ed. J. R. Durig, Vol. 6; Marcel Dekker, 1977; chapter 1.
[82] M. Abd El Rahim, R. Antoine, M. Broyer, D. Rayane, and P. Dugourd, *J. Phys. Chem. A*, 2005, **109**, 8507–8514.
[83] J. K. G. Watson, *Can. J. Phys*, 1975, **53**, 2210–2220.
[84] P. R. Bunker and P. Jensen, *Molecular Symmetry and Spectroscopy*, NRC Research Press, Ottawa, Ontario, Canada, 2 ed., 1998.
[85] S. C. Wang, *Phys. Rev.*, 1929, **34**, 243.
[86] J. Küpper and F. Filsinger, `libcoldmol`: A particle trajectory calculation framework, 2003-2008.
[87] D. C. Lainé and R. Sweeting, *Phys. Lett. A*, 1971, **34**, 144.
[88] J. C. Helmer, F. B. Jacobus, and P. A. Sturrock, *J. Appl. Phys.*, 1960, **31**, 458.
[89] Nevertheless, the focusing of molecules in hfs states has been demonstrated using cylindrical capacitors with a central wire[87] and arrays of crossed wires.[88]
[90] Interesting enough these studies were performed at the *Kaiser Wilhelm Institut für physikalische Chemie und Elektrochemie*, the predecessor of the Fritz Haber Institut in Berlin.
[91] A similar field could, of course, be created by applying dc voltages in a quadrupole arrangement of ±0.6 kV, although the trap depth and characteristics would be different due to the approximately quadratic Stark effect of NH_3 at the resulting low field strengths.